

Article

# Power Quality Enhancement in a Grid-Integrated Photovoltaic System Using Hybrid Techniques

Prasad Kumar Bandahalli Mallappa \*, Herminio Martinez Garcia and Guillermo Velasco Quesada

Department of Electronic Engineering, Eastern Barcelona School of Engineering (EEBE), Technical University of Catalonia-BarcelonaTech (UPC), Eduard Maristany Ave 16, E-08019 Barcelona, Spain; herminio.martinez@upc.edu (H.M.G.); guillermo.velasco@upc.edu (G.V.Q.)

\* Correspondence: prasad.kumar.bandahalli@upc.edu

**Abstract:** In recent years, the photovoltaic (PV) system was designed to supply solar power through photovoltaic arrays. The PV generator exhibits nonlinear voltage–current characteristics and its maximum power point tracking (MPPT), which varies with temperature and radiation. In the event of non-uniform solar insolation, several multiple maximum power points (MPPs) appear in the power–voltage characteristic of the PV module. Thus, a hybrid combination of binary particle swarm optimization (BPSO) and grey wolf optimization (GWO) is proposed herein to handle multiple MPPs. This combination is nowhere found in the literature, so the author chose this hybrid technique; and the main advantage of the proposed method is its ability to predict the global MPP (GMPP) in a very short time and to maintain accurate performance, even under different environmental conditions. Moreover, a 31-level multilevel inverter (MLI) was designed with a lower blocking voltage process to reduce the complexity of the circuit design. The entire system was executed in the MATLAB platform to examine the performance of the PV system, which was shown to extract a maximum power of 92.930 kW. The simulation design clearly showed that the proposed method with a 31-level MLI achieved better results in terms of total harmonic distortion (THD) at 1.60%, which is less when compared to the existing genetic algorithm (GA) and artificial neural networks (ANNs).

**Keywords:** photovoltaic; maximum power point tracking; grey wolf optimization; binary particle swarm optimization; multilevel inverter; total harmonic distortion

**Citation:** Bandahalli Mallappa, P.K.; Garcia, H.M.; Quesada, G.V. Power Quality Enhancement in a Grid-Integrated Photovoltaic System Using Hybrid Techniques. *Appl. Sci.* **2021**, *11*, 10120. <https://doi.org/10.3390/app112110120>

Academic Editors: Pawel Szcześniak and Piotr Lezynski

Received: 17 September 2021

Accepted: 23 October 2021

Published: 28 October 2021

**Publisher's Note:** MDPI stays neutral with regard to jurisdictional claims in published maps and institutional affiliations.



**Copyright:** © 2021 by the authors. Licensee MDPI, Basel, Switzerland. This article is an open access article distributed under the terms and conditions of the Creative Commons Attribution (CC BY) license (<https://creativecommons.org/licenses/by/4.0/>).

## 1. Introduction

Solar energy is an inexhaustible and less-polluting energy resource that has received widespread attention in renewable energy production. Photovoltaic power generation is an effective method for using solar energy [1]. In recent years, most research works have concentrated on extracting more power, which can be achieved effectively from PV cells [2]. In comparison to other renewable energy sources, solar PV is a natural energy source that is more efficient because it is free, clean, and abundant [3]. The energy consumption of the PV system has been reduced by effectively designing MPPT [4]. The nonlinear characteristic of PV cell output is not only affected by the temperature, but also by the load when the light intensity is fixed [5]. This paper presents some efficient ideas to improve the performance of MPPT. In the past few years, several MPPT techniques have been implemented, but still, some enhancements are required in MPPT to improve the PQ features.

PV cells allow energy to be carried by electromagnetic waves, which have to be converted into electricity [6]. The MPPT technique implemented in the PV system creates full utilization of the PV array output power and it tracks the efficient MPP from the PV array input. The major challenge of the MPPT technique is automatically detecting the voltage

or current MPP [7, 8]. Changes in the output voltage can impact MPPT's output characteristics [9]. However, the existing inverter levels provide some inaccuracy, because they require additional functionalities. The time required to predict GMPP strictly depends on the number of PV arrays and the complexity of the system design [9, 10].

To overcome the above-discussed issues, the currently exploited novel optimization is required. Hence, a hybrid BPSO–GWO-based PV system that is connected to the grid is introduced to enhance the power quality (PQ) features. Maximum power transfer from the PV array to the grid is ensured using BPSO. The proposed MPPT technique provides highly efficient performance with a quick response under variable climate conditions, and in the case of a sudden variation in irradiance level. This research investigates a hybrid control scheme to grant multiple functions to a grid-connected PV inverter. This strategy guarantees a constant energy supply independently of the intermittent nature of solar energy. The main advantages of this proposed method are fast MPPT performance and less complexity than the Gauss–Newton, because double derivative terms are not present in the hybrid algorithm.

The organization of this paper is as follows: Section 2 provides a literature review relevant to this work. The problem statement and its objectives are explained in Sections 3 and 4, respectively. Section 6 describes the workflow of the proposed method. Section 7 provides the results and discussions of the BPSO–GWO method. Finally, the conclusion is explained in Section 8.

## 2. Literature Review

Kollimalla et al. [11] demonstrated a variable P&O MPPT algorithm that was implemented to track the MPP during sudden changes in irradiance. This technique includes three algorithms, namely, the current perturbation algorithm, the adaptive control algorithm, and the variable perturbation algorithm. The variable perturbation algorithm dynamically decreases the perturbation size, which is completely based on the polarity of the change in power, but it requires a large data storage area and extensive computation.

Elmetennani et al. [12] presented the MPPT technique, implemented using a hybrid dynamical technique to model the PV generator. The designed MPPT algorithm for optimization of the PV chain production is used to monitor the functionality of each power conductor device. The designed MPPT structure uses a multicellular converter instead of a classic DC/DC converter to overcome the properties of its specific topology. The design of the MPPT algorithm is completely suitable for multiple-cell structures, but the same procedure was not followed when designing the N-cell structure.

Keyrouz [13] demonstrated an intelligent Bayesian network (BN) method used for MPP tracking of a PV array under partial shading conditions (PSCs). This method achieves efficient performance in terms of robustness, tracking efficiency, and speed, which was demonstrated through different simulated scenarios. In the proposed method, the PV array is desired to operate at any time period. In this proposed algorithm, the additional computational burden on the processor is added, whereas an enormous number of particles is required to cover the entire system.

Robles Algarín et al. [14] presented a fuzzy controller for tracking the MPP to improve the PQ features. This research developed an optimal MPPT technique that was tested under varying climatic conditions. This method can supply the maximum possible power to a battery in an off-grid PV system using a fuzzy controller. The proposed technique uses simpler hardware setup throughout, where only one voltage sensor is utilized. A closed-loop MPPT technique was developed based on a conventional PI controller, although the fuzzy controllers used in the method are very expensive.

Koad et al. [15] demonstrated a new MPPT technique that implements a PV system based on the PSO algorithm and the Lagrange interpolation formula. Here, the proposed PSO shows better results because of its simple implementation and capability to achieve

MPP in various environmental circumstances. An optimum number of iterations is required to achieve the MPP, but it is difficult to detect the resulting power loss and convergence issues.

Several works are reported in the literature, as this area has attracted considerable interest from the research community compared to other optimization techniques, because it is more robust and exhibits faster convergence. Furthermore, it requires fewer parameters for adjustment and fewer operators compared to other evolutionary approaches, which is an advantage when a rapid design process is considered. After a thorough literature survey, it was observed that the hybrid combination of BPSO–GWO has not been exploited for designing an MPPT. Hence, this work attempted to exploit the BPSO–GWO for designing an MPPT to obtain efficient tracking performance of a PV system under various conditions.

### 3. Problem Identification

- The random nature of the solar array generates fluctuations in electric power. These fluctuations harm the stability and power quality of electric power systems.
- Due to the high penetration level of solar energy in distribution systems, the utility (grid) is of high concern, because it provides a threat to the entire system in terms of THD, voltage regulation, and stability.
- To develop an innovative and integrated approach using optimization techniques that enhance the power quality of solar power systems.
- In all conditions, the main purpose of PV with an additional inverter topology is to develop energy savings, along with excellent service. The challenging tasks for this type of system design are:
  - An appropriate multilevel inverter topology.
  - A control strategy for the PV generator.

### 4. Objectives

- In this research, a combination of the BPSO and GWO methods with a boost converter is proposed to control the MPPT of the PV array.
- The output of the BPSO–GWO generates the value of the duty cycle (D). In order to achieve a better THD, the value of the duty cycle should be adjusted accordingly.
- To design a 31-level multilevel inverter for the PV system. Similarly, PWM pulses are produced from the control algorithm, which are given to the multilevel inverter.
- To analyze the capability of MPPT tracking and the efficiency of the inverter at different irradiation conditions, a hybrid combination of BPSO and GWO is proposed.

The objective of the present study is to provide technical analysis of a grid-connected PV system in power quality of distribution network with emphasis on THD. This research will also propose two solutions for overcoming the high THD for the period PV system operation. Connecting inverters to the utility grid results in frequency fluctuations, harmonic distortion and power factor degradation. The proposed BPSO–GWO is used to enlighten both the power generation and THD in the present system which is described clearly in the upcoming sections.

### 5. Modeling of the PV Array

The number of PV modules is optimized to reduce the cost of energy, which covers the load demand. Additionally, the output power of the PV module is mainly based on the temperature, manufacturing characteristics, and geographical locations. The PV system voltage and capacity are determined by connecting the PV panel either in parallel or in a series connection [16]. The MPPT method is considered in the PV system to increase the PV output power. Table 1 clearly depicts the specific value of parameters of the PV array of the module.

**Table 1.** Specification of the PV array.

Parameters	Value
The voltage at maximum power point, $V_{mp}$	54.7 V
Temperature coefficient of $V_{oc}$	-0.27269 (%/deg.C)
Temperature coefficient of $I_{sc}$	0.061745 (%/deg.C)
Shunt resistance	269.5934 ohms
Short-circuit current, $I_{sc}$	5.96 A
Series resistance	0.37152 ohms
Open circuit voltage, $V_{oc}$	64.2 V
Maximum power	305.226 W
Light generated current, $I_L$	6.0092 A
Diode saturation current	0.000063*10 <sup>-5</sup> A
Diode ideality factor	0.94504
Current at maximum power point of $I_{sc}$	5.58 A

Equation (1) is used to identify the output power that depends on the  $I_M$  and  $V_M$ , which denote the maximum current and voltage, respectively.

$$P_{MPPT}(t) = I_{MPPT}(t) \times V_{MPPT}(t) \tag{1}$$

The current and voltage of MPPT are given in Equations (2) and (3), respectively.

$$I_{MPPT}(t) = I_{SC} \left\{ 1 - C_1 \left[ \exp \left( \frac{V_M}{C_2 \times V_{OC}} \right) \right] \right\} + \Delta I(t) \tag{2}$$

$$V_{MPPT}(t) = V_M + \mu V_{OC} \cdot \Delta T(t) \tag{3}$$

where the short circuit current is represented as  $I_{SC}$ ;  $C_1$ , and  $C_2$  are the capacitances;  $V_M$  is the maximum voltage; and the open circuit voltage is represented as  $V_{OC}$ .

$C_1$ ,  $C_2$ ,  $\Delta I(t)$ , and  $\Delta T(t)$  of Equations (2) and (3) are expressed in Equations (4)–(7), respectively.

$$C_1 = \left( 1 - \frac{I_M}{I_{SC}} \right) \times \exp \left( - \frac{V_M}{C_2 \times V_{OC}} \right) \tag{4}$$

$$C_2 = \left( \frac{V_M}{V_{OC}} - 1 \right) \times \left[ \ln \left( 1 - \frac{I_M}{I_{SC}} \right) \right]^{-1} \tag{5}$$

$$\Delta I(t) = I_{SC} \left( \frac{GT(t)}{G_{ref}} - 1 \right) + \alpha_{1,sc} \times \Delta T(t) \tag{6}$$

$$\Delta T(t) = T_c(t) - T_{c,ref} \tag{7}$$

The  $I_M$  is the maximum current, the incident radiation on the PV surface is represented as  $GT(t)$ , and  $\alpha_{1,sc}$  signifies the constant value during short-circuit operation. The cell temperature is represented as  $T_c$ , and the PV temperature in the standard condition is represented as  $T_{c,ref}$ . The MPPT technique computes the panel operating voltage and current period (POVCP) and measures the instantaneous power. The efficiency of the MPPT technique is improved by minimizing the steady-state oscillation and eliminating the variable irradiance level. The dynamic perturbation step size is used to minimize the oscillation, whereas boundary conditions are introduced to avoid the diverging characteristic of MPP. The general block diagram of the MPPT technique is shown in Figure 1.

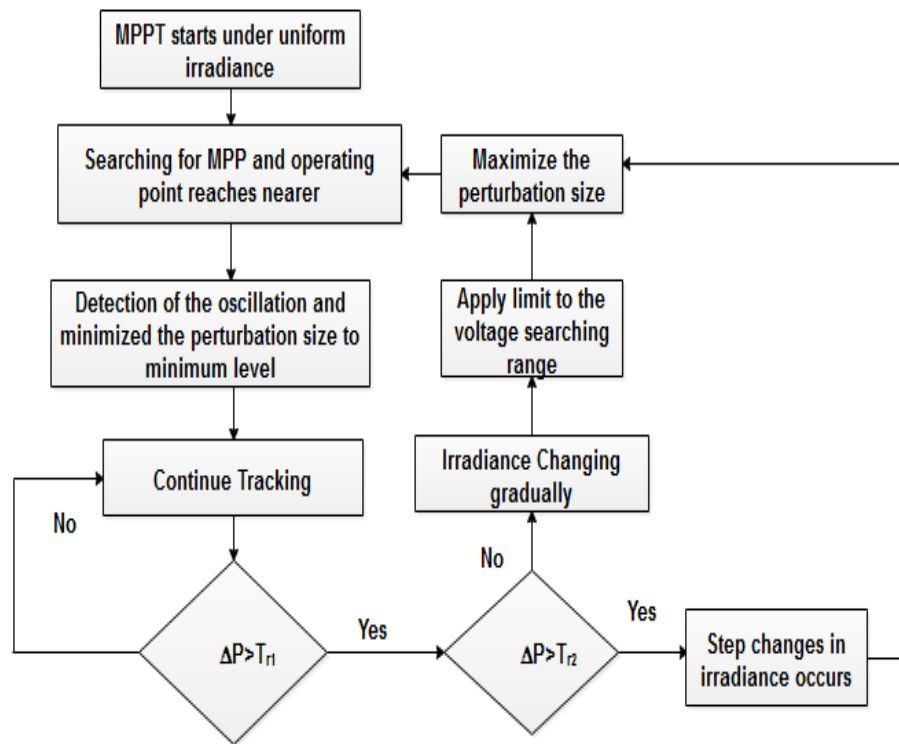
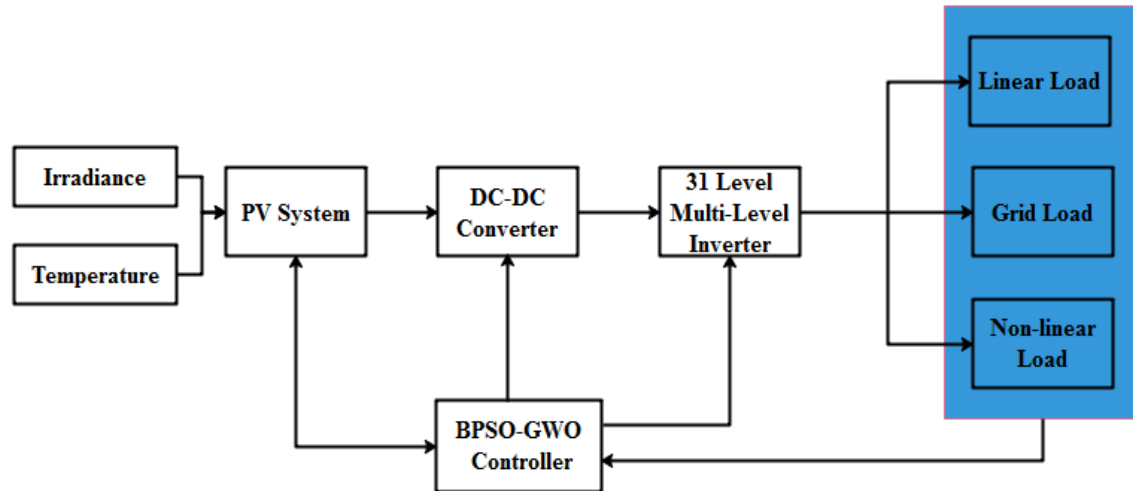


Figure 1. General flow of the MPPT technique.

Similarly, the operating point of MPP oscillates around the consecutive samples. However, the oscillation is found by a special mechanism and the perturbation size is minimized until it achieves a positive minimum value [17]. Here, less power tolerance is allowed to handle the small flickers that occur in the power issue. The consecutive samples have a difference in power ( $\Delta P$ ), due to the small oscillations. The size of perturbation achieves a minimum value because the  $\Delta P/P$  value is maintained below the threshold limit ( $T_{r1}$ ).

### 6. Proposed Method

Under various environments, the unshaded PV array obtains high irradiation, whereas the shaded portion collects less irradiation only. The partial condition is characterized by the amount of shaded portion, and its shading factor is defined as the ratio of irradiation on the shaded modules to the unshaded modules. If the partial working condition is detected, then the condition is fully considered by assuming the shading factor. Proper recognition and detailed valuation of partial shading are necessary for MPPT to demand the correct procedure and to track the MPP. The block diagram of a PV system under various loads is shown in Figure 2.



**Figure 2.** Block diagram of the proposed method under various loads.

### 6.1. 31-Level Multi-Level Inverter

This research recommends a new configuration for a 31-level MLI using a reduced maximum blocking voltage procedure. This process provides several levels with the smallest number of power electronic buttons. The main advantages of the proposed design are as follows: decrements in the installation area, switches count, power diodes, gate driver circuits, and cost. The implemented procedure supports controlling the extent of DC sources [18]. This calculation is presented to define the optimum dc voltage ratio for the MLI that determines the number of voltage levels that are accessible for the ensuing high PQ. The Simulink structure for the 31-level MLI with the blocking voltage process is shown in Figure 3. In Figure 3, MOSFET SL3 uses the P-Channel MOSFET as the charge carrier, which has less mobility than electron flow.

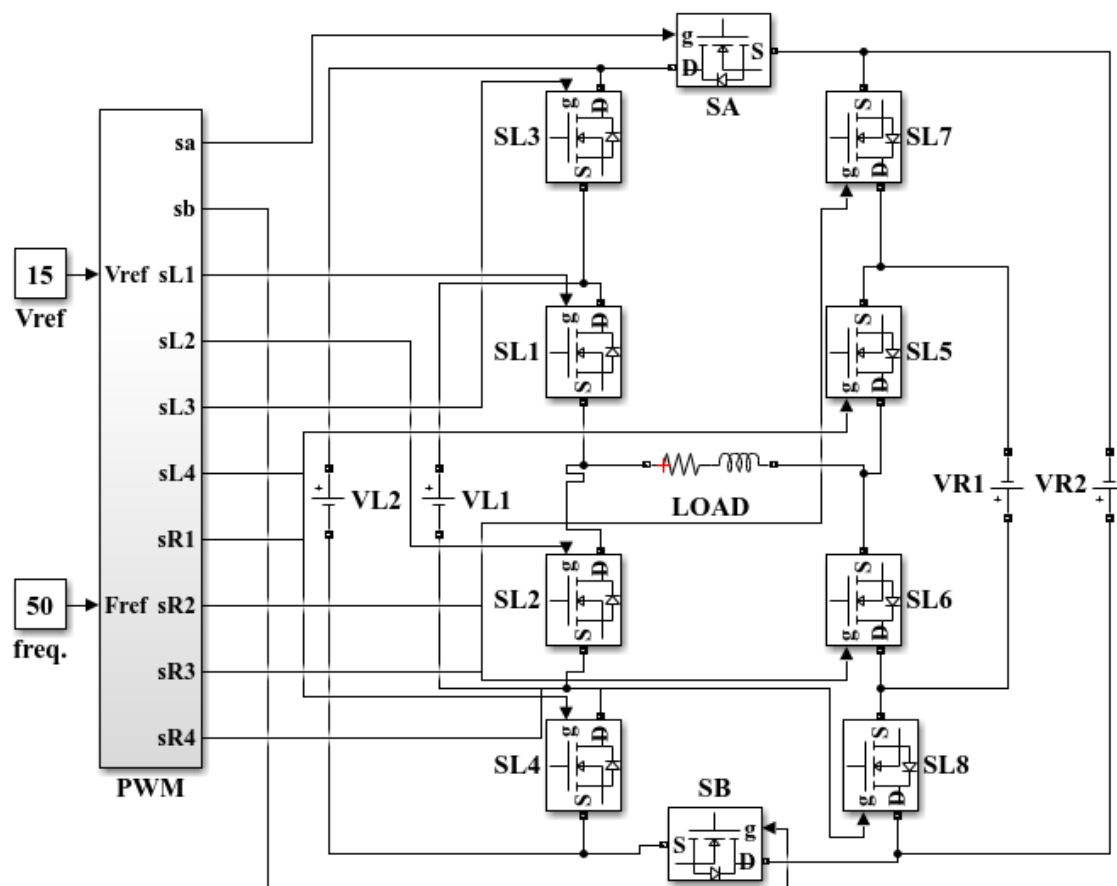


Figure 3. Structure of the 31-level MLI with the blocking voltage process.

Due to achieving the maximum power from PV panels subjected to non-uniform solar irradiances, such as PSCs, a new evolutionary computing technique, i.e., grey wolf optimization, was employed to design a global MPPT. This BPSO–GWO method was employed in a simulation, and it was found that it is very efficient at providing a maximum power yield from PV panels under non-uniform solar irradiances.

### 6.2. Preliminaries

In this study, the DC/AC and DC/DC converters were controlled using the proposed BPSO–GWO algorithm. This algorithm is very easy to implement with less adjusting parameters, and it is effective for integrating PV into the grid to attain smooth power quality. Moreover, it is a superior fitness solution with good convergence speed, and the response of the controller was studied under constant temperature and changing irradiance. The results show the proficiency of the proposed controller at improving the performance of the system.

### 6.3. Binary Particle Swarm Optimization

Initially, the global MPPT technique was carried out by using the BPSO method, in order to overcome mismatching phenomena problems related to partial shading. The BPSO-based MPPT technique performance was always able to reach the GMPP, allowing the increase in the PV system efficiency. The input for the proposed BPSO calculates the PV power and its rate of conversion, where the change in reference current is referred to as the output. The GWO algorithm is used in the implementation of the MPPT method [19]. BPSO is the combination utilized to monitor the global MPP (GMPP) of the PV. The BPSO technique is used to attain the maximum global point, which exploits the maximum

power extracted in the PV arrangements. In BPSO, the bit string and velocity of the particle are created in the range of [0, 1]. The velocity of the particle is defined as the bit possibility to obtain a value of 1. The BPSO is considered an adequate algorithm to enhance the efficiency of the distribution system.

$X_k^i$  and  $V_k^i$  represent the particle's position and the velocity at the  $k^{th}$  iteration, respectively. The  $i^{th}$  particle's velocity at the iteration  $k + 1$  is calculated using Equation (8).

$$V_{k+1}^i = \omega \cdot V_k^i + C1 \cdot R1 (P_{best} - X_k^i) + C2 \cdot R2 (G_{best} - X_k^i) \quad (8)$$

where the random values are represented as  $R1$  and  $R2$ , and the inertia weight factor is represented as  $\omega$ , which is expressed in Equation (9).

$$\omega = \omega_{max} - \{(\omega_{max} - \omega_{min}) - k_{max}\} \times k \quad (9)$$

where the maximum amount of iteration considered for BPSO is  $k_{max}$ . Moreover, the particle's position is updated by adding the previous position and current velocity value, which is shown in Equation (10).

$$X_{k+1}^i = X_k^i + V_{k+1}^i \quad (10)$$

The swarm expression of particles is retained, which is unchanged in BPSO. The logistic transformation  $S(V_k^i)$  is utilized to accomplish the modification, as shown in Equations (11) and (12).

$$S(V_{k+1}^i) = \text{sig mod } e(V_{k+1}^i) = \frac{1}{1 + \exp(V_{k+1}^i)} \quad (11)$$

$$\text{If rand} < S(V_{k+1}^i) \text{ then: } X_{k+1}^i = 1; \quad (12)$$

$$\text{Else: } X_{k+1}^i = 0;$$

where the sigmoid limiting transformation is represented as  $S(V_k^i)$  and the quasi-random value selected among [0, 1] is represented as  $rand$ . Figure 4 shows the flowchart for the proposed BPSO–GWO method.



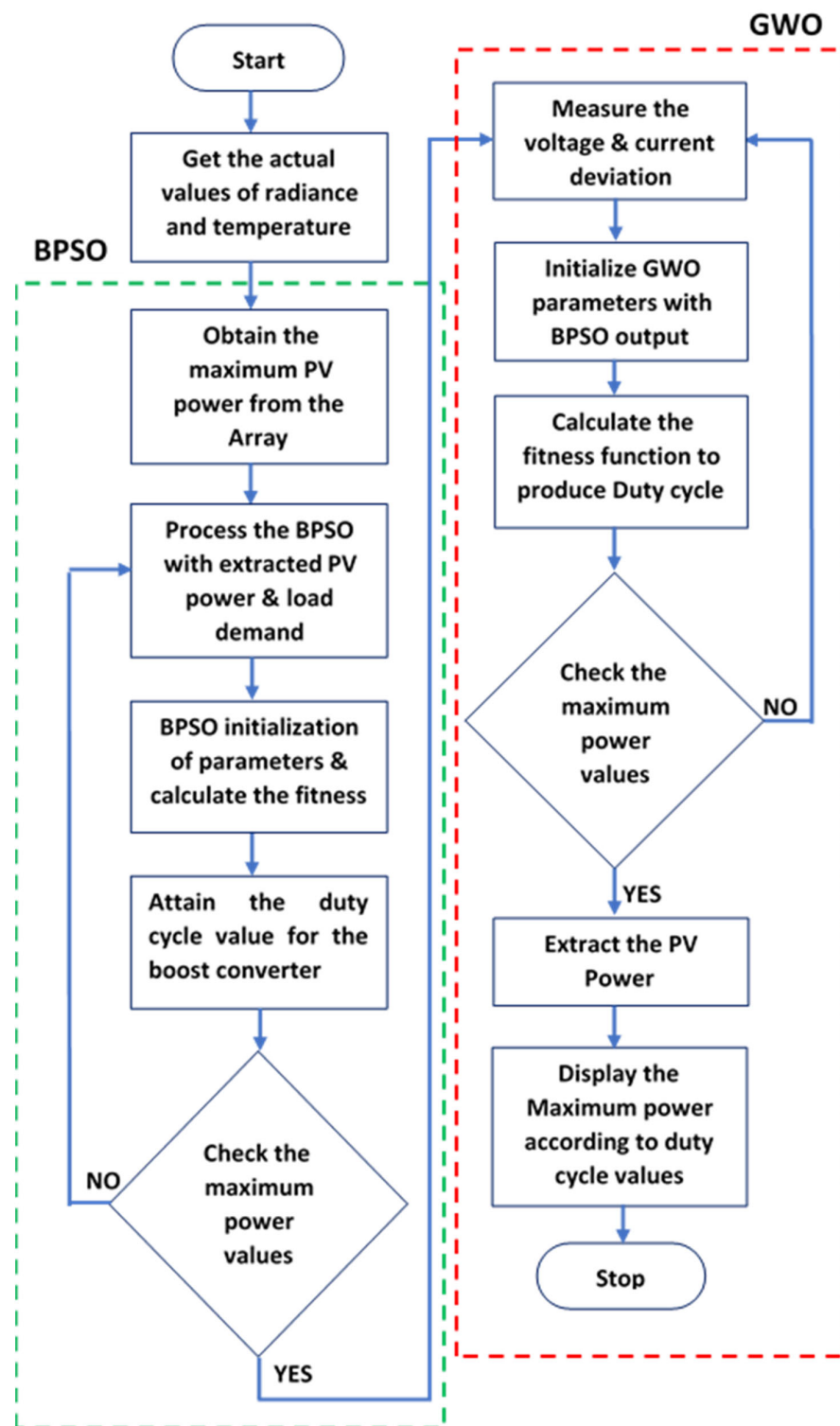


Figure 4. Flowchart of the proposed BPSO–GWO method.

#### 6.4. Grey Wolf Optimization

In order to overcome this obstacle (MPP), the grey wolf optimization (GWO) method is proposed in order to track the global maximum power point and to maximize the en-

ergy extraction of the PV system. During improper irradiation, the P–V curve is categorized by multiple peaks with various local peaks (LPs) and one global peak (GP). It is noteworthy that when the wolves find the MPP, their correlated coefficient vectors become nearly equal to zero. In the proposed method, an attempt was made to combine GWO with duty-cycle control; i.e., at the MPP, the duty cycle is sustained at a constant value, which in turn reduces the steady-state oscillations that exist in conventional MPPT techniques, and lastly, the power loss due to oscillation is reduced, resulting in higher system efficiency. To implement the GWO-based MPPT, the duty cycle  $D$  is defined as a grey wolf.

GWO is generally inspired by the leadership and hunting behavior of the grey wolves. The grey wolves are categorized into four levels based on the social dominance hierarchy, namely, alpha wolf ( $\alpha$ ), beta wolf ( $\beta$ ), delta wolf ( $\delta$ ), and omega wolf ( $\omega$ ). Generally, the GWO depends on the following assumptions: (1)  $\alpha$ ,  $\beta$ , and  $\delta$  denote the optimum, second optimum, and third optimum solutions, respectively. (2) The remaining level is supposed to be the omega wolf ( $\omega$ ). (3) The three wolves' alpha, beta, and delta are considered the optimum solutions with better information about the potential location of prey. The information about prey is known by the three wolves, in that the alpha wolf knows much better than the remaining two wolves. (4) The omega wolf follows the three best wolves. The global best position ( $gbest$ ) from the AHCS is considered a location vector of prey [20]. The process of GWO is given as follows:

a. Encircling prey

Equation (13) defines the encircling behavior of grey wolves.

$$Y^{t+1} = Y_p^t - B^t \times |D^t \times Y_p^t - Y^t| \tag{13}$$

where the prey's location vector is represented as  $Y_p^t$ , the coefficient vectors are  $B^t$  and  $D^t$ , and the grey wolf's position vector is  $Y^t$ . Equations (14) and (15) are represented as the coefficient vector of  $B^t$  and  $D^t$ , respectively.

$$B^t = 2b^t rand_1 - b^t \tag{14}$$

$$D^t = 2rand_2 \tag{15}$$

where the exploration rate is specified as  $b^t$ , and  $rand_1$  and  $rand_2$  represent the random vectors among 0 and 1. The exploration rate is linearly minimized from 2 to 0 over the number of iterations. The exploration rate is specified in Equation (16).

$$b_j^t = 2 - \frac{2t}{N_{max}} \tag{16}$$

where  $N_{max}$  specifies the maximum number of iterations.

b. Hunting

The hunting process of grey wolves is handled by the alpha wolf. Sometimes, the remaining beta and delta wolves contribute as guides during the hunting period. However, it is very difficult to obtain the prey location in a search space. The three wolves, alpha, beta, and delta, have better information about the potential location of prey. These prey locations are used to process the hunting behavior of grey wolves. Equations (17)–(19) are used to stimulate the hunting process of the GWO.

$$Y_1 = Y_\alpha^t - B_1^t \times |D_1^t \times Y_\alpha^t - Y^t| \tag{17}$$

$$Y_2 = Y_\beta^t - B_2^t \times |D_2^t \times Y_\beta^t - Y^t| \tag{18}$$

$$Y_3 = Y_\delta^t - B_3^t \times |D_3^t \times Y_\delta^t - Y^t| \tag{19}$$

where  $Y_\alpha^t$ ,  $Y_\beta^t$ , and  $Y_\delta^t$  are the positions of the alpha, beta, and delta wolves, respectively. The average states of the positions obtained from the alpha, beta, and delta wolves are

given in Equation (20). The average position provides the optimum position of the grey wolf.

$$Y^{t+1} = \frac{Y_1 + Y_2 + Y_3}{3} \tag{20}$$

For the GWO, the convergence factor is linearly dropped from 2 to 0 through the iteration count. Meanwhile, the PV array’s output power similarly fluctuates once the outside atmosphere changes. To avoid the procedure dropping into an infinite sequence, it is essential to start again the procedure for tracking the power. Once the output power difference is fulfilled, the procedure is re-initialized, which is stated in Equation (21).

$$\left| \frac{P_{real} - P_m}{P_m} \right| > \Delta P \tag{21}$$

where the actual output power is stated as  $P_{real}$ , the PV output power is represented as  $P_m$ , and the threshold for the output power change is expressed as  $\Delta P$ , which is fixed as 0.2. The duty cycle equation is written as (13):

$$D_i(k + 1) = D_i(k) - B^t H^t \tag{22}$$

where  $D_i(k + 1) = \text{new duty cycle value}$ . The controller architecture designed in this PV system is given in Figure 5. In Figure 5,  $I_a, I_b,$  and  $I_c$  represent the current that occurs at three phase sources.  $V_{IsQ}$  States the instantaneous shunt voltage at the quadrature axis. The error attained between the reference current and the actual current is fed into the BPSO–GWO controller to produce the direct axis current  $I_d^*$ . Then, the quadrature axis current  $I_q^*$  is set as zero, because it is responsible for reactive power. The output current is then compared to the actual current supplied to the electrical grid.

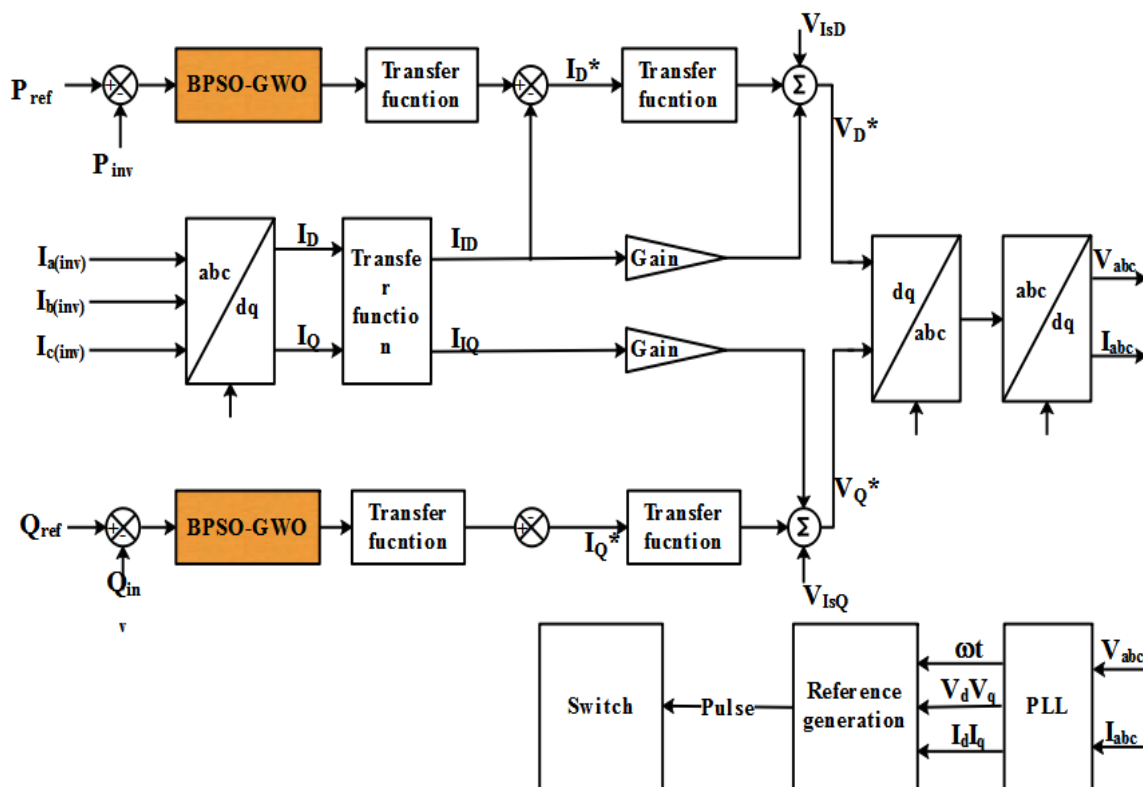


Figure 5. Control circuit diagram of the proposed method.

The aim of the controller, as shown in Figure 5, is to transfer all the active power produced by the PV system to the grid, and also to produce a nil amount of reactive power so that unity power factor is obtained, except when the grid operator requires reactive power. The error attained between the reference current and actual current is fed into the BPSO–GWO controller to produce direct axis current  $I_d^*$ . Then, the quadrature axis current,  $I_q^*$ , is set to be zero because it is responsible for reactive power. The output current is then compared to the actual current supplied to the electrical grid. The error difference between the two signals is connected to the current control, which produces the gate signal. The same process is evaluated for the voltage control loop also. Then, the phase locked loop (PLL) is used to synchronize the three-phase voltage with the current. From the calculated voltage and current, switching pulses are created which are used to trigger the switches present in the multilevel inverter.

### Fitness Function Derivation

The derivation of the fitness function for the proposed BPSO–GWO method is outlined in this section. Thus, the fitness function of the proposed algorithm is formulated as Equation (23).

$$Pd_k^i > Pd_k^{i-1} \tag{23}$$

where  $P$  represents the power,  $d$  is the duty cycle,  $i$  is the number of current grey wolves, and  $k$  is the number of iterations.

### 7. Results and Discussion

The implementation of the proposed method was carried out using the MATLAB/Simulink platform. In this research, the designed PV model was named Sun Power (SPR 305W). This portion demonstrates the outcomes of the simulation, connected through the PV module, which operates with the proposed BPSO–GWO algorithm to extract the maximum power. The grid-tied PV system was modeled, and the PQ was analyzed using the BPSO–GWO optimization technique. The proposed method controls the duty ratio of the boost converter to enhance the power quality. Figure 6 illustrates the Simulink model of the proposed method with the 31-level MLI.

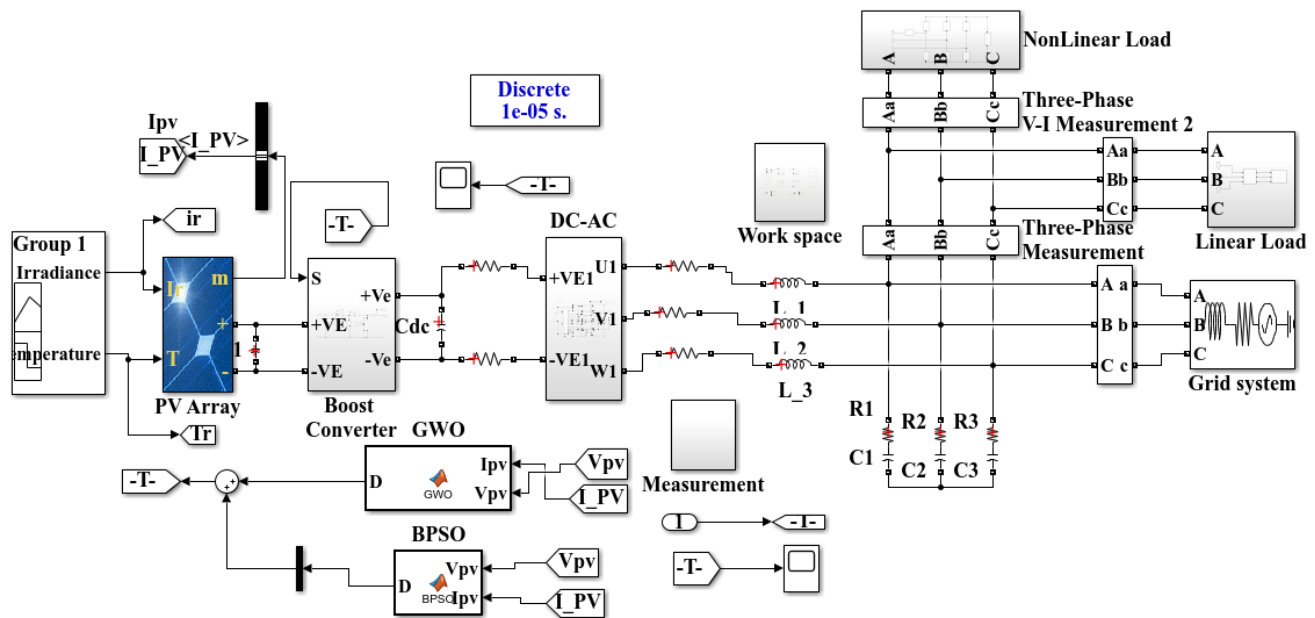


Figure 6. Simulink diagram of the proposed method.

This paper presents some efficient ideas to improve the performance of MPPT. To date, several MPPT techniques have been implemented, but still, there are some improvements required in MPPT to achieve maximum efficiency. This research concluded that the proposed BPSO–GWO technique performs well during uniform solar irradiance (SI). Figures 7–9 clearly show that the proposed method extracted maximum power when compared to other MPPT algorithms, which are shown in the below figures. The figures clearly explain the concept of PV power tracking with respect to irradiance and temperature; meanwhile, the dc link voltage and duty cycle values are also displayed therein.

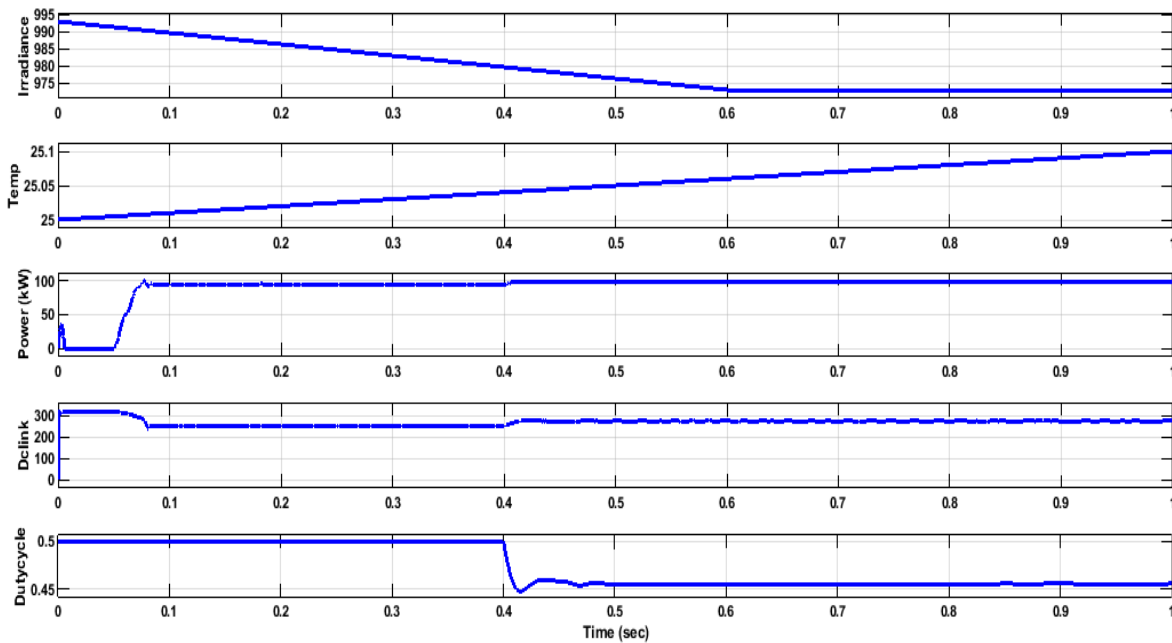


Figure 7. PV performance factors measured using the BPSO method.

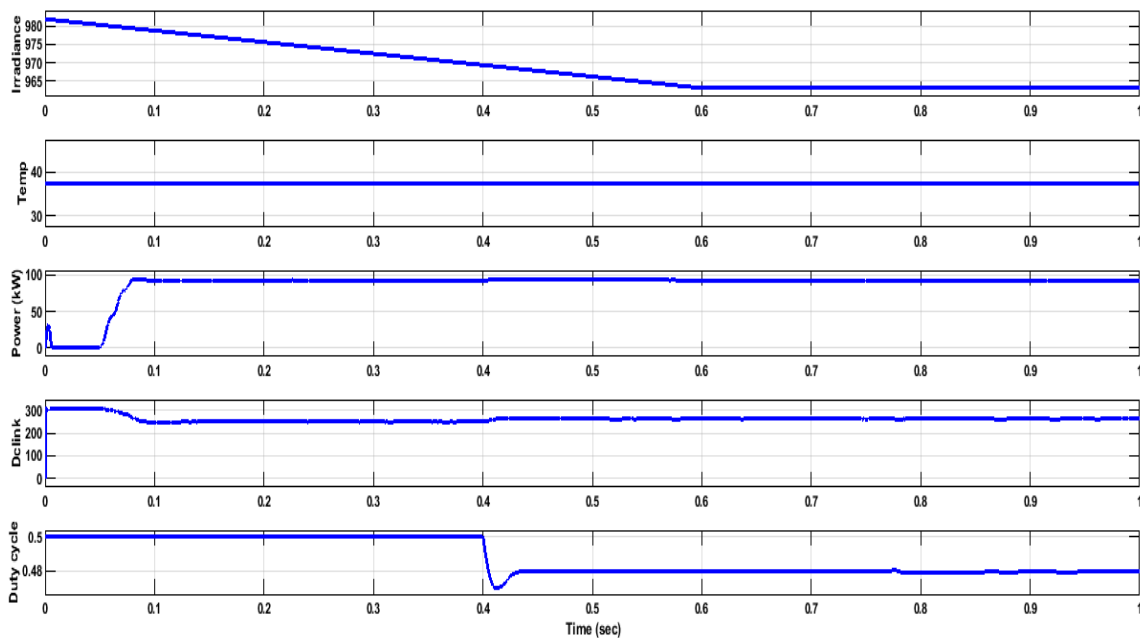


Figure 8. PV performance factors measured using the GWO method.

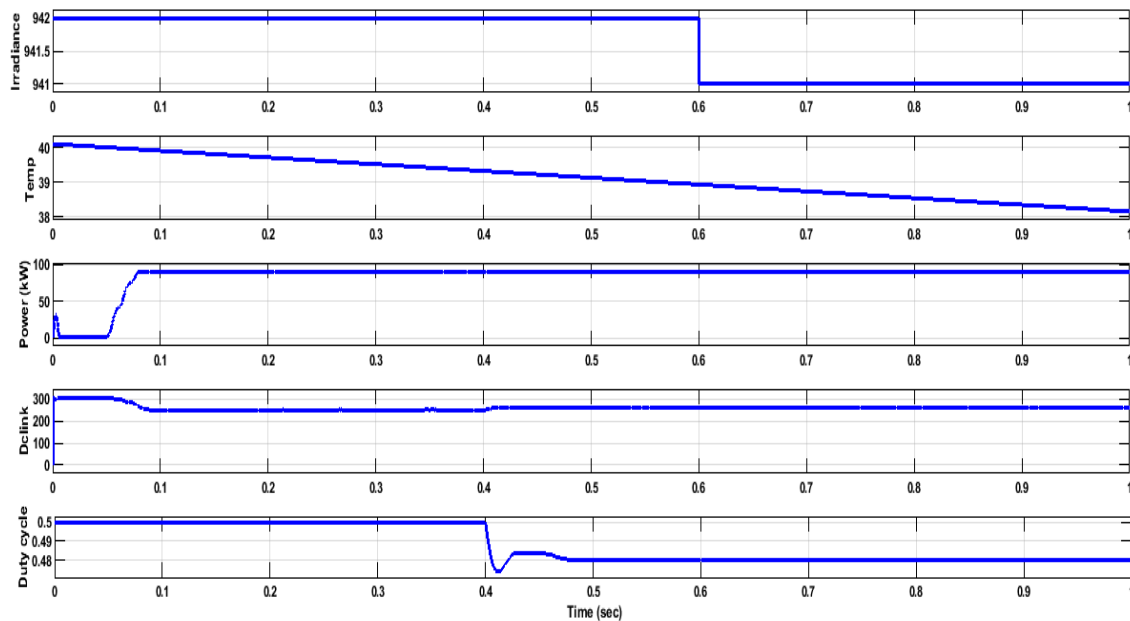


Figure 9. PV performance factors measured using the BPSO–GWO method.

Figure 10 illustrates the comparative analysis of PV power using various techniques. Table 2 indicates that the proposed BPSO–GWO technique achieved the maximum power of 92.930 kW, which is better than the independently exploited BPSO and GWO techniques. Table 2 clearly shows that the BPSO and GWO extracted the maximum power levels of 88.209 and 90.238 kW, respectively.

Table 2. Comparison of PV power under linear load.

Techniques	PV Power (kW)
BPSO method	88.209
GWO method	90.238
Proposed BPSO–GWO method	92.930

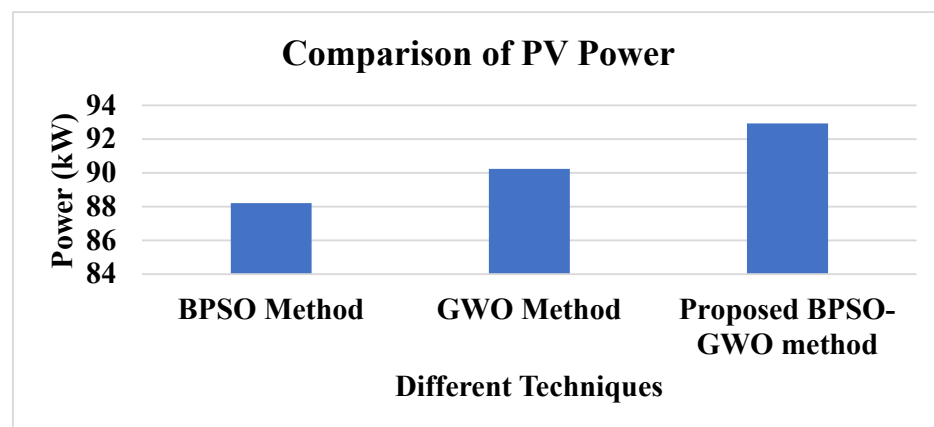


Figure 10. THD analysis of the 31-level MLI.

Figures 11 and 12 provide the output FFT investigation for the PV system under different loads through the BPSO–GWO technique. Figure 9 demonstrates that the 31-level MLI with the voltage blocking process achieved a 3.70% THD. A similar concept combined with the proposed BPSO–GWO under different loads attained a THD of 1.60%. The

following table displays the simulated outcomes attained by the FFT investigation of the output waveform for linear, nonlinear, and grid loads by means of BPSO–GWO. Table 3 tabulates the analysis of the 31-level MLI with the proposed BPSO–GWO controller.

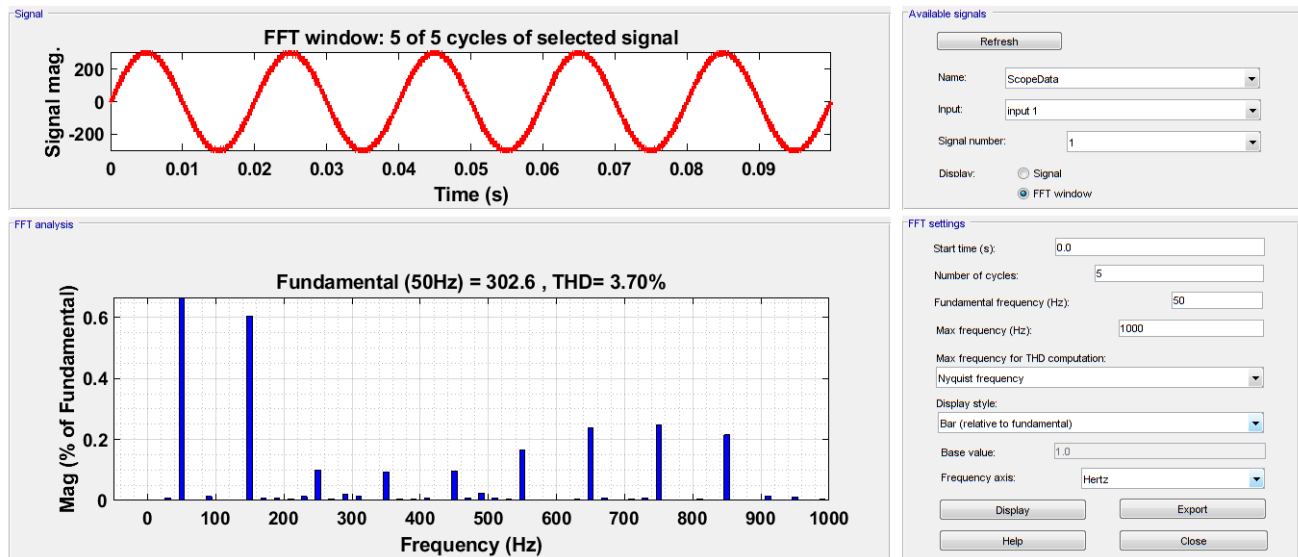


Figure 11. THD analysis of the 31-level MLI.

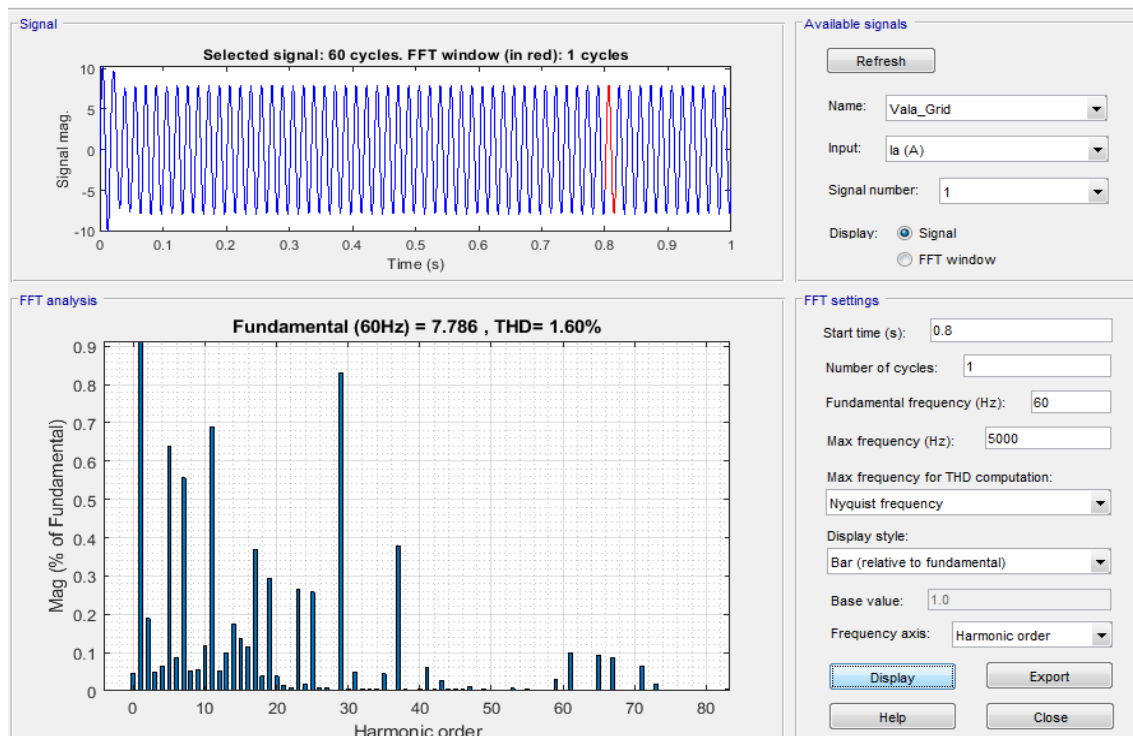


Figure 12. FFT investigation of the 31-level MLI with BPSO–GWO.

Table 3. FFT analysis of the 31-level MLI.

Techniques	THD (%)
31-level MLI without a controller	3.70

31-level MLI with the hybrid BPSO–GWO controller	1.60
--	------

**THD Analysis under Linear and Nonlinear Loads**

The THD analysis of the 31-level multilevel inverter with the proposed BPSO–GWO method under various loads, namely, linear, nonlinear, and grid loads, is tabulated in Table 4 below. Table 4 clearly indicates that the proposed BPSO–GWO method achieved a better THD of 1.60%, which is much better when compared to other existing methods such as the genetic algorithm (5.13%) and artificial neural networks (2.86%) [16].

**Table 4.** Comparison of the FFT analysis.

Techniques	THD (%)
Genetic algorithm [16]	5.13
Artificial neural networks [16]	2.86
BPSO controller	3.12
GWO controller	2.28
Hybrid BPSO–GWO controller	1.60

Figure 13 illustrates the THD values for the 31-level MLI, and Table 4 explains the THD analysis for the MLI with different techniques. From the simulation results, it can be concluded that the proposed BPSO–GWO technique achieved less THD in the 31-level MLI blocking voltage process compared to the genetic algorithm and artificial neural network techniques.

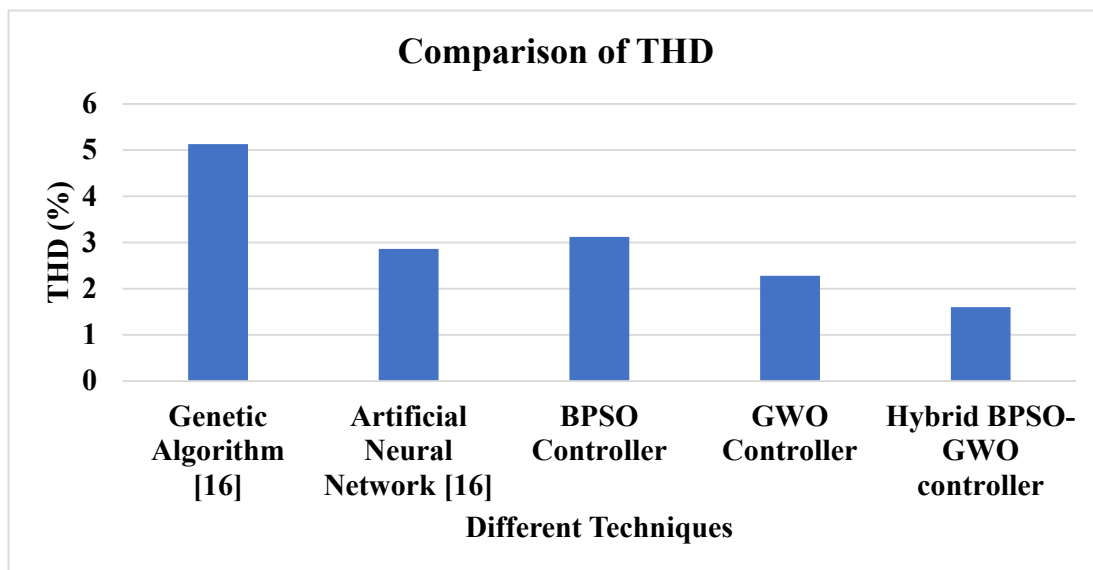


**Figure 13.** Graphical analysis of the THD performance.

**8. Conclusions**

For the past few years, several MPPTs, such as hill climbing, perturb and observe, and incremental conductance, have been proposed. However, these techniques do not consider partial shading conditions or the stochastic nature of solar insolation. To identify the maximum power in PV, it is necessary to implement the MPPT technique in the PV system, which dynamically adjusts the extraction of power. Herein, the hybrid combination of BPSO–GWO was proposed, and the convergence speed was shown to be a significant characteristic of this technique. In this research, GWO handled the initial stages of MPP tracking, followed by the application of BPSO in the final stage because of achieving



faster convergence of the global peak. Furthermore, a 31-level MLI was designed with a blocking voltage process that reduces the complexity of the entire system. The results clearly showed that the proposed BPSO–GWO method could attain less THD (1.60%), than the existing techniques. We achieved a maximum power of 92.930 kW from the solar PV panel with the help of the BPSO–GWO method. Furthermore, the experimental validation of the proposed method will be taken into account in the future. In the future, this research could be extended with other novel hybrid techniques, along with different configurations of MLI to improve the power quality features.

**Author Contributions:** Conceptualization, P.K.B.M., H.M.G., and G.V.Q.; methodology, P.K.B.M., H.M.G., and G.V.Q.; software, P.K.B.M.; validation, P.K.B.M.; formal analysis, P.K.B.M.; investigation, P.K.B.M., H.M.G., and G.V.Q.; resources, H.M.G. and G.V.Q.; writing—original draft preparation, P.K.B.M.; writing—review and editing, H.M.G. and G.V.Q.; visualization, P.K.B.M.; supervision, H.M.G. and G.V.Q.; project administration, H.M.G. and G.V.Q.; funding acquisition, H.M.G. and G.V.Q. All authors have read and agreed to the published version of the manuscript.

**Funding:** This research was funded by MCIN/ AEI /10.13039/501100011033/ and by ERDF. ERDF a way of making Europe thanks to grant PGC2018-098946-B-I00. The APC was funded by grant PGC2018-098946-B-I00 funded by: MCIN/ AEI /10.13039/501100011033/ and by ERDF A way of making Europe.

**Acknowledgments:** The authors would like to thank the Spanish Ministerio de Ciencia, Innovación y Universidades (MICINN)-Agencia Estatal de Investigación (AEI) and the European Regional Development Funds (ERDF), by grant PGC2018-098946-B-I00 funded by MCIN/ AEI /10.13039/501100011033/ and by ERDF.ERDF A way of making Europe.

**Institutional Review Board Statement:** Not applicable.

**Informed Consent Statement:** Informed consent was obtained from all subjects involved in the study.

**Data Availability Statement:** The data presented in this study are available on request from the corresponding authors.

**Conflicts of Interest:** The authors declare no conflict of interest.

### Table of Nomenclature

$V_{OC}$	Open circuit voltage
$I_{SC}$	Short circuit current
$I_{MPPT}$	MPPT current
$V_{MPPT}$	MPPT voltage
$V_M$	Maximum voltage
$C_1$ and $C_2$	Capacitances
$P_{MPPT}$	Maximum power
$\Delta T$	Change in temperature
$I_M$	Maximum current
$T_c$	Cell temperature
$X_k^i$	Particle position
$V_k^i$	Velocity
$R1$ and $R2$	Random values
$P_{best}$	Personal best
$G_{best}$	Global best
$\Omega$	Inertia weight
$S(V_k^i)$	Sigmoid limiting transformation
$Y^t$	Grey wolf's position vector
$Y_p^t$	Prey's location vector
$\alpha$	Alpha wolf
$\beta$	Beta wolf
$\delta$	Delta wolf
$\omega$	Omega wolf

$B^t$ and $D^t$ ;	Coefficient vectors
$b^t$ .	Exploration rate
$Y_\alpha^t, Y_\beta^t$ and $Y_\delta^t$	Position of the alpha, beta, and delta wolves
$N_{max}$	Maximum number of iterations
$Y^{t+1}$	Average position
$f_i$	Best fitness value

## References

- Zhou, Y.; Li, H. Analysis and suppression of leakage current in cascaded-multilevel-inverter-based PV systems. *IEEE Trans. Power Electron.* **2013**, *29*, 5265–5277.
- Jain, S.; Venu, S. A highly efficient and reliable inverter configuration based cascaded multilevel inverter for PV systems. *IEEE Trans. Ind. Electron.* **2016**, *64*, 2865–2875.
- Das, M.K.; Jana, K.C.; Akanksha, S. Performance evaluation of an asymmetrical reduced switched multi-level inverter for a grid-connected PV system. *IET Renew. Power Gener.* **2013**, *12*, 252–263.
- Sumit, K.C.; Chandan, C. A new asymmetric multilevel inverter topology suitable for solar PV applications with varying irradiance. *IEEE Trans. Sustain. Energy* **2017**, *8*, 1496–1506.
- Rajalakshmi, S.; Parthasarathy, R. Investigation of modified multilevel inverter topology for PV system. *Microprocess. Microsyst.* **2019**, *71*, 102870.
- Jahan, H.K.; Abapour, M.; Zare, K.; Hosseini, S.H.; Blaabjerg, F.; Yang, Y. A Multilevel Inverter with Minimized Components Featuring Self-balancing and Boosting Capabilities for PV Applications. *IEEE J. Emerg. Sel. Top. Power Electron.* **2019**, *1*, doi:10.1109/jestpe.2019.2922415.
- Bana, P.R.; Kaibalya, P.P.; Sanjeevikumar, P.; Mihet-Popa, L.; Panda, G.; Wu, J. Closed-loop control and performance evaluation of reduced part count multilevel inverter interfacing grid-connected PV system. *IEEE Access* **2020**, *8*, 75691–75701.
- Ahmed, A.; Mohan, S.M.; Joung-Hu, P. An efficient single-sourced asymmetrical cascaded multilevel inverter with reduced leakage current suitable for single-stage PV systems. *IEEE Trans. Energy Convers* **2018**, *34*, 211–220.
- Lingom, P.M.; Song-Manguelle, J.; Mon-Nzongo, D.L.; Costa Flesch, R.C.; Jin, T. Analysis and control of PV cascaded H-bridge multilevel inverter with failed cells and changing meteorological conditions. *IEEE Trans. Power Electron.* **2020**, *36*, 1777–1789.
- Manoharan, M.S.; Ashraf, A.; Joung-Hu, P. A PV power conditioning system using nonregenerative single-sourced trinary asymmetric multilevel inverter with hybrid control scheme and reduced leakage current. *IEEE Trans. Power Electron.* **2016**, *32*, 7602–7614.
- Kollimalla, S.K.; Mishra, M.K. Variable perturbation size adaptive P&O MPPT algorithm for sudden changes in irradiance. *IEEE Trans. Sustain. Energy* **2014**, *5*, 718–728.
- Elmetennani, S.; Laleg-Kirati, T.M.; Djemai, M.; Tadjine, M. New MPPT algorithm for PV applications based on hybrid dynamical approach. *J. Process. Control.* **2016**, *48*, 14–24.
- Keyrouz, F. Enhanced Bayesian Based MPPT Controller for PV Systems. *IEEE Power Energy Technol. Syst. J.* **2018**, *5*, 11–17.
- Robles, A.; Carlos, J.T.G.; Omar, R.A. Fuzzy logic based MPPT controller for a PV system. *Energies* **2017**, *10*, 2036.
- Koad, R.B.A.; Ahmed, F.Z.; El-Shahat, A. A novel MPPT algorithm based on particle swarm optimization for photovoltaic systems. *IEEE Trans. Sustain. Energy* **2017**, *8*, 468–476.
- Atiq, J.; Soori, P.K. Modelling of a grid connected solar PV system using MATLAB/Simulink. *Int. J. Simul. Syst. Sci. Technol.* **2017**, *17*, 45.1–45.7.
- Hariri, M.H.M.; Desa, M.K.M.; Masri, S.; Zainuri, M.A.A.M. Grid-Connected PV Generation System—Components and Challenges: A Review. *Energies* **2020**, *13*, 4279, doi: 10.3390/en13174279.
- Shankar, J.G.; Belwin Edward, J.; Sathish Kumar, K.; Jaocb Raglend, I. A 31-level asymmetrical cascaded multilevel inverter with DC-DC flyback converter for photovoltaic system. In Proceedings of the 2017 International Conference on High Voltage Engineering and Power Systems (ICHVEPS), Denpasar, Indonesia, 2–5 October 2017; pp. 277–282.
- Abdulkadir, M.; Yatim, A.H.; Yusuf, S.T. An Improved PSO-Based MPPT Control Strategy for Photovoltaic Systems. *Int. J. Photoenergy* **2014**, *2014*, 1–11, doi:10.1155/2014/818232.
- Almutairi, A.; Abo-Khalil, A.; Sayed, K.; Albagami, N. MPPT for a PV Grid-Connected System to Improve Efficiency under Partial Shading Conditions. *Sustainability* **2020**, *12*, 10310, doi: 10.3390/su122410310.